RIETI Discussion Paper Series 21-E-005

Money Flow Network Among Firms' Accounts in a Regional Bank of Japan

FUJIWARA, Yoshi
University of Hyogo

INOUE, Hiroyasu
University of Hyogo

YAMAGUCHI, Takayuki
Shiga University

AOYAMA, Hideaki
RIETI

TANAKA, Takuma
Shiga University

KIKUCHI, Kentaro
Shiga University

RIETI
Research Institute of Economy, Trade & Industry, IAA

The Research Institute of Economy, Trade and Industry
https://www.rieti.go.jp/en/

RIETI Discussion Paper Series 21-E-005
January 2021

Money flow network among firms' accounts in a regional bank of Japan[1]

Yoshi FUJIWARA[1,2], Hiroyasu INOUE[1], Takayuki YAMAGUCHI[2],
Hideaki AOYAMA[3,4], Takuma TANAKA[5], Kentaro KIKUCHI[6]
[1]Graduate School of Simulation Studies, University of Hyogo
[2]The Center for Data Science Education and Research, Shiga University
[3]Research Institute of Economy, Trade and Industry, [4]RIKEN iTHEMS,
[5]Graduate School of Data Science, Shiga University, [6]Faculty of Economics, Shiga University

Abstract

In this study, we investigate the flow of money among bank accounts possessed by firms in a single region by employing an exhaustive list of all the bank transfers in a regional bank in Japan, to clarify how the network of money flow is related to the economic activities of the firms. The network statistics and structures are examined and shown to be similar to those of a nationwide production network. Specifically, the bowtie analysis indicates what we refer to as a "walnut" structure with core and upstream/downstream components. To quantify the location of an individual account in the network, we used the Hodge decomposition method and found that the Hodge potential of the account has a significant correlation to its position in the bowtie structure as well as to its net flow of incoming and outgoing money and links, namely the net demand/supply of individual accounts. In addition, we used non-negative matrix factorization to identify important factors underlying the entire flow of money; it can be interpreted that these factors are associated with regional economic activities. One factor has a feature whereby the remittance source is localized to the largest city in the region, while the destination is scattered. The other factors correspond to the economic activities specific to different local places. This study serves as a basis for further investigation on the relationship between money flow and economic activities of firms.

Keywords: bank remittance, Hodge decomposition, non-negative matrix factorization, bowtie structure, complex network

JEL classification: E00, E40, C00, C02

[1]This study is conducted as a part of the Project “Macro-Economy under COVID-19 influence: Data-intensive analysis and the road to recovery” undertaken at the Research Institute of Economy, Trade and Industry (RIETI). The authors are grateful to Shiga Bank, Ltd. for giving us an opportunity to study such a unique and valuable dataset. They are also grateful to Yoshiaki Nakagawa (The Center for Data Science Education and Research, Shiga University) and Discussion Paper seminar participants at RIETI for helpful discussions.

1 Introduction

Determining how money flows among economic entities is an important aspect of understanding the underlying economic activities. For example, the so-called flow of funds accounts record the financial transactions and the resulting credits and liabilities among households, firms, banks, and the government (see, e.g., [1]). Another example is the input-output table, which describes the purchase and sale relationships among producers and consumers within an economy and clarifies the flows of final and intermediate goods and services with respect to industrial sectors and product outputs (e.g., [2]). These data are used in macroscopic studies, such as those of industrial sectors and aggregated economic entities.

Recent years have witnessed the increasing emergence of microscopic data. For example, one can study a nationwide production network, i.e., how individual firms transfer money among one another as suppliers and customers for transactions of goods and services (see [3] and the references therein). In contrast to the macroscopic studies mentioned above, microscopic studies can uncover the heterogeneous structure of the network and its role in economic activities, how the activities are subject to shocks due to natural disasters [4] and pandemics [5], and so forth. However, microscopic data are not exhaustive; although they may cover most active firms, not all the suppliers and customers are recorded. Such records are based on a survey in which a firm nominates a selected number of important customers and suppliers. In addition, the transaction amounts are often lacking; hence, the network is directed but only binary. More importantly, microscopic and macroscopic data are compiled and updated annually or quarterly at most (see [3, 6] and the references therein).

To uncover how economic entities such as firms perform economic activities in a real economy, we should ideally study how money flows among firms by using real-time data of bank transfers with exhaustive lists of accounts and transfers. Also, investigating money flows among accounts will help to tackle real-world problems including the prediction of the economic impact of COVID-19, the defaults of firms, and the bank accounts that could be involved in illegal activities. However, these problems have been addressed without utilizing the information about the network of money flow [7]. The prediction accuracy will be improved by taking into account the network as well as other features. To the best of our knowledge, such a study has not been conducted thus far, simply because such data are not available for academic purposes. The present study precisely performs such an analysis of a Japanese bank's dataset. The bank is a regional bank, which has a high market share with respect to the loans and deposits in a prefecture, particularly supporting financial transactions among the manufacturing firms located there (according to a disclosure issued by the bank).

The objective of this study is to investigate economic activities via bank transfers among firms' accounts by selecting all the transfers related to the firms to uncover how money flows behind the economic activities. More specifically, we examine the network and flow structures, especially the so-called bowtie structure, to locate the position of individual accounts upstream and downstream of the entire flow. We quantify the location using the method of Hodge decomposition of the flow. Furthermore, we examine geographical information of bank transfers in order to see how geographical relations between remittance

source and destination are represented by a small number of components of areas.

2 Data

Our dataset comprises all the bank transfers that are sent from or received by the bank accounts in a regional bank. The regional bank is Shiga Bank, Ltd., the largest bank in a prefecture in Japan, which is mid-sized in terms of its population (more than a million) and economic activity. All the accounts are anonymous for obvious reasons, while several attributes such as geographical locations are given to the accounts owned by firms under the anonymity. Hereafter, we refer to it simply as Bank A for brevity. The period covered in our study is from March 1, 2017, to July 31, 2019, i.e., a period of 29 months or 883 days.

During this period, there were 23 million transfers among 1.7 million bank accounts involving a total of 17.4 trillion yen (roughly 160 billion USD or 140 billion Euros). Let us denote a transfer from account i to account j by $i \to j$. To focus only on the firms' accounts in Bank A, we filtered the data such that (i) both i and j are the accounts of Bank A, (ii) both i and j are owned by firms excluding households, and (iii) self-loops $i \to i$ are deleted. Point (ii) is important for our purpose, because our concern here is how money flows and circulates among firms' accounts, which is considered to be closely related to the firms' economic activities. The resulting data are summarized in Table 1 (see the rightmost column).

Table 1: **Bank accounts and transfers: summary**

Number/Amount	**Entire data**	**Within Bank A**	
		all	firms
#Accounts	1.71 M	642,411	30,613
#Transfers	23.06 M	12,847,963	2,409,619
#Links	3.13 M	1,470,107	280,864
Transfer (Yen)	17.43 T	5.26 T	2.15 T

For a transfer $i \to j$, the column "Entire data" includes the cases in which either i or j is not an account of Bank A. The column "Within Bank A" corresponds to the case in which both i and j are accounts of Bank A. "firms" implies that both the source and the target of a link are firm accounts. M and T denote million and trillion, respectively.

Note that multiple transfers $i \to j$ can exist for a given pair of i and j, because of frequent transfers. One can quantify the strength of the directional relationship between a pair of accounts either by the flow of transfers or by their frequency. To do so, we aggregate multiple transfers, if present, into a single link $i \to j$ with two types of weights, namely flow f_{ij} and frequency g_{ij} (see the illustration in Fig. 1). Hereafter, we use the term *link* for aggregated transfers.

The number of accounts or nodes in the network is $N = 30,613$, while the number of links is $M = 280,864$ after the aggregation (see Table 1).

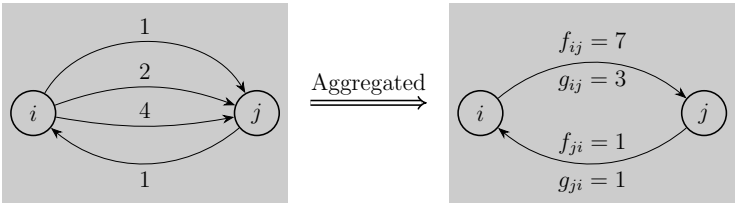

Figure 1: **Construction of bank-transfer network by aggregation.** How bank transfers are aggregated into links. i made three transfers (1, 2, and 4) in an arbitrary unit of money to j, while j made one transfer (1) to i during a certain period. Flow f_{ij} is defined by the total flow of transfers along $i \to j$. Frequency g_{ij} is the frequency of these transfers.

The summary statistics of the links' flows f_{ij} and frequencies g_{ij} for all the pairs of accounts i and j are presented in Table 2. One can observe that the distributions for flow and frequency have large skewness, implying that a considerable fraction of the money flow is due to a large amount transferred by a small number of flows.

Table 2: **Summary statistics for links' flows and frequencies**

Stats.	**Flow (Yen)**	**Frequency**
Min.	1	1
Max.	3.00×10^{10}	2,616
Median	0.20×10^{6}	3
Avg.	7.65×10^{6}	8.58
Std.	1.53×10^{8}	19.92
Skewness	92.5	37.8
Kurtosis	1.25×10^{4}	3.49×10^{3}

Summary statistics of the links' flows and frequencies for all the pairs of accounts, where links are aggregated transfers as defined in the main text and Fig. 1.

3 Results and Discussion

3.1 Network of firms' accounts and links of transfers

First, let us summarize the network structure comprising firms' accounts as nodes and aggregated transfers as links. We remark that transfers are aggregated into links as shown in Fig. 1. The degree is the number of transfers received by or sent from an account. The number of incoming and outgoing links of an account is called the in-degree and out-degree, respectively. Fig. 2 shows the distributions of the in-degree and out-degree as complementary cumulative distributions. By noting that the total number of accounts is $N = 30,613$, we can see that a small fraction of accounts has a considerable degree, i.e., a thousand or more links, while most accounts have a limited number of links.

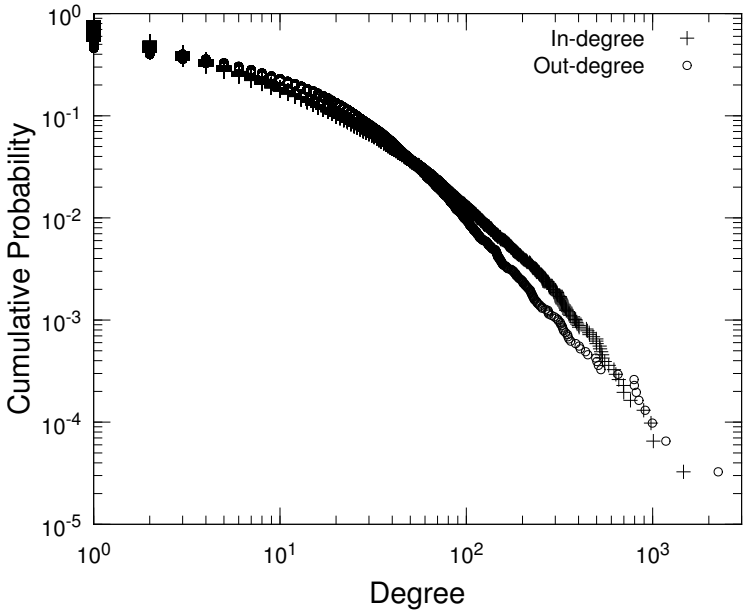

Figure 2: **Degree distributions for the bank transfer network.** Complementary cumulative distributions for in-degree and out-degree, which refer to the number of incoming and outgoing links, respectively, of each account.

Such hubs are presumably entities associated with the local government or the public sector in the region.

Because each node has an in-degree and out-degree, we can examine how they are correlated. Fig. 3 shows the scatter plot for the in-degree and out-degree of each account. We can observe a tendency for a positive correlation between the degrees (Pearson's $r = 0.303$ ($p < 10^{-6}$); Kendall's $\tau = 0.164$ ($p < 10^{-6}$)). We also observe that there are accounts that have many more incoming links than outgoing ones (and vice versa), which can be respectively considered as "sinks" and "sources" with respect to the money flow. If household accounts were included, one would have a larger number of sinks corresponding to the situation that income and saving are likely larger than expenditure and dissaving, but such sinks are not present here.

We can observe each link's weights, flow f_{ij}, and frequency g_{ij} (see Fig. 1). Fig. 4 shows the complementary cumulative distribution for the flow along each link. The distribution is highly skewed; there exist a small number of links that have a large amount of flow exceeding a billion yen — likely important channels with large flows of money. Quantitatively, 0.1% of the links have flows larger than a billion yen.

Fig. 5 shows the complementary cumulative distribution for the frequency along each link. The steps at 30 and 60 on the horizontal axis are considered to correspond to transfers performed once or twice in each month (recall that the entire period includes 29 months). We can see that 0.1% of the links have frequencies of 500 or more corresponding to daily transfers on weekdays.

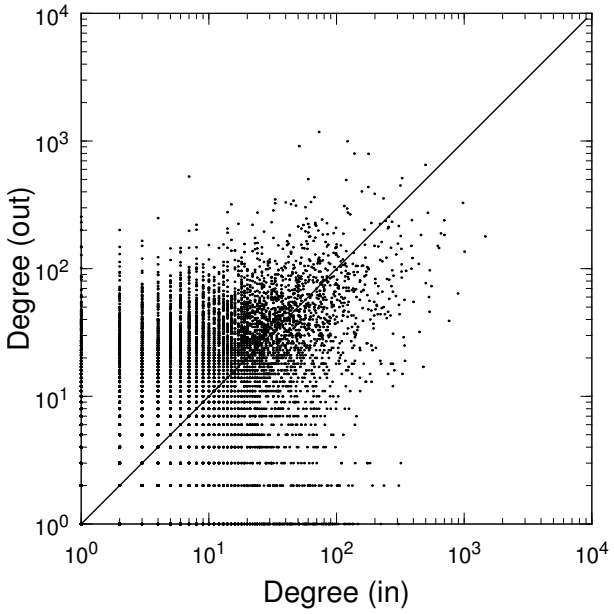

Figure 3: **Scatter plot for in-degree and out-degree of each account.** Each account as a node, represented as a point, has incoming links and outgoing links, the numbers of which are represented by the horizontal and vertical axes, respectively. The diagonal line represents the locations where the in-degree and out-degree are equal.

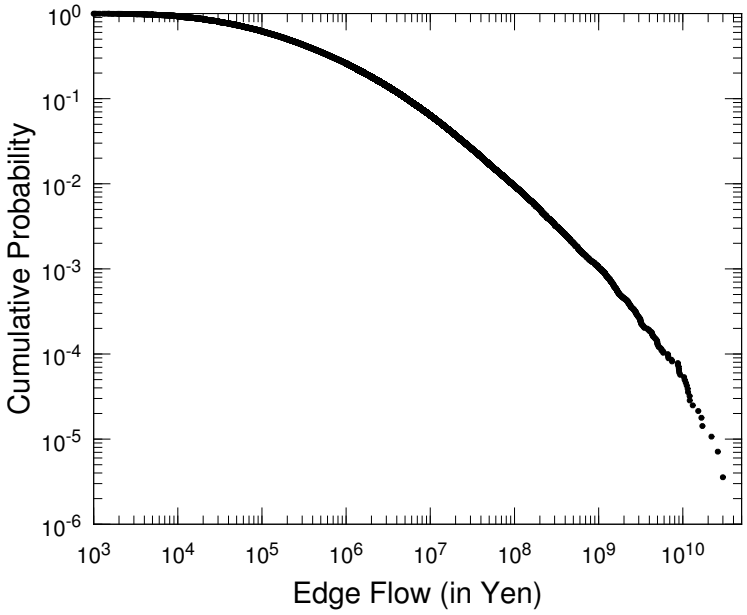

Figure 4: **Distribution for the flows of links.** Complementary cumulative distributions for the amount of money defined by f_{ij} between each pair of accounts i and j (see Fig. 1).

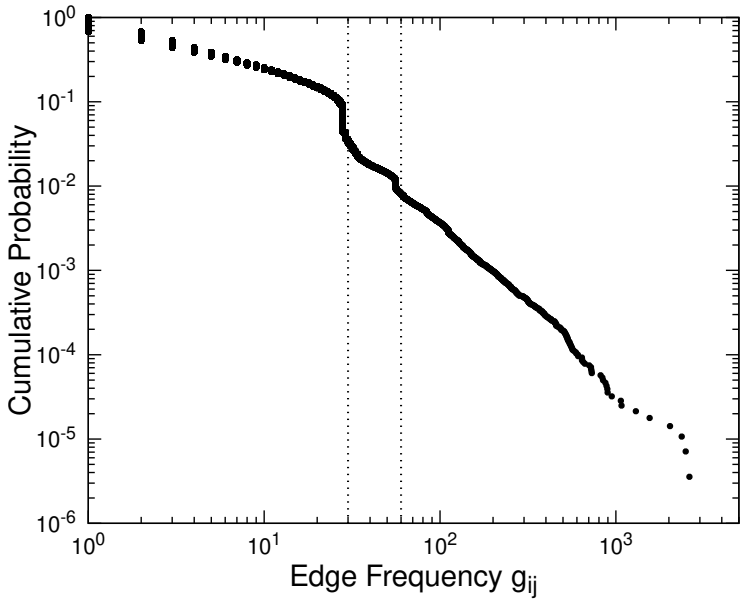

Figure 5: **Distribution for the frequencies of transfers.** Complementary cumulative distributions for the frequency defined by g_{ij} between each pair of accounts i and j (see Fig. 1). We can observe that there are frequency steps around 30 and 60 (vertical dotted lines), which are presumed as periodic transfers performed once or twice in each month (recall that the entire period includes 29 months).

3.2 Community analysis

Communities or clusters in a network are tightly knit groups with high intra-group density and low inter-group connectivity [8]. Community analysis is useful for understanding how a network has such heterogeneous structures. We adopt the widely used Infomap method [9, 10] to detect communities in our data.

The results are presented in Table 3. "Level" indicates the level of communities in a hierarchical tree of communities that are detected recursively (see [10]). The number of communities indicates how many communities are detected at the corresponding level. The label "irr. comm." denotes irreducible communities that cannot be decomposed further to the next level of smaller communities in the hierarchical decomposition. For example, 143 of 164 communities at the first level are irreducible ones, whereas the rest of them are decomposed into 2,327 smaller communities at the next level, and so forth.

Table 3: **Numbers of communities, irreducible communities, and accounts at each level of community analysis using Infomap**

Level	**#comm.**	**#irr. comm.**	**#accounts**	**Ration(%)**
1	164	143	355	0.012
2	2,327	2,264	28,948	94.5
3	215	215	1,310	0.043
Total	—	2,621	30,613	100.0

Each level corresponds to the hierarchical level in the Infomap community analysis [10]. A community at a level can be decomposed at the next lower level (from top to bottom). If a community cannot be decomposed further, it is called an irreducible community. The numbers of irreducible communities are listed in the third column. The fourth column lists the numbers of accounts belonging to these irreducible communities at each level.

We find that most of the communities are at the second level because of the number of accounts, and that most of the accounts (94.5%) belong to the second-level communities. In our previous study [11] on the application of hierarchical community analysis using Infomap to a large-scale production network, we showed that a relatively shallow hierarchy can be observed at the fifth level as the lowest level; in particular, most firms are included at the second level, exactly as we find here. This is reasonable, because our data on bank transfers among firms' accounts should reflect a regional fraction of the entire production network on a nationwide scale. The finding here is interesting, because this implies a self-similar structure of the production network meaning that a partial system has a similar network property to the global system.

Fig. 6 shows the distribution of the sizes of irreducible communities at the lowest level that includes all the accounts. The size of a community is simply the number of nodes included in the community. The result indicates that the size of the communities is highly skewed over a few orders of magnitude. We note that there exist more than 10 communities with sizes exceeding 100, which correspond to important clusters of economic activities that depend on geographical sub-regions and industrial sectors. We shall discuss this issue in our analysis of non-negative matrix factorization later.

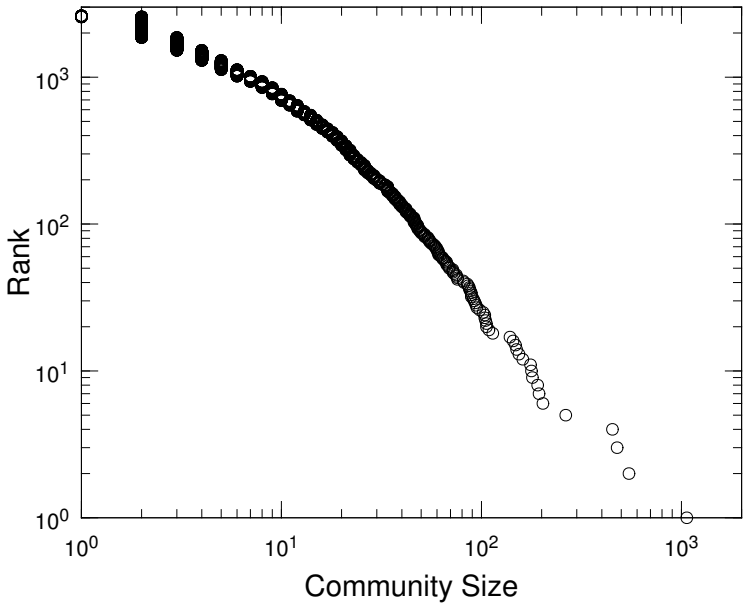

Figure 6: **Distributions of the sizes of irreducible communities.** Rank-size plot for the sizes of irreducible communities detected using the Infomap method at all the levels, where the ranks are in descending order of the size with the lowest rank equal to the total number of irreducible communities (see Table 3). The size of a community is simply the number of nodes included in the community.

3.3 Bowtie structure

With respect to the flow of money, the accounts can be located in a classification of the so-called *bowtie* structure, which was first adopted in the study of the Internet [12]. In the context of economics and finance, the method has been applied to business relationship networks [13] and credit default swap network [14], for example. Nodes in a directed network can be classified into a giant strongly connected component (GSCC), its upstream side as the IN component, its downstream side as the OUT component, and the rest of the nodes that do not belong to any of GSCC, IN, and OUT. In general, they can be defined as follows.

GWCC Giant weakly connected component: the largest connected component when viewed as an undirected graph. At least one undirected path exists for an arbitrary pair of nodes in the component.

GSCC Giant strongly connected component: the largest connected component when viewed as a directed graph. At least one directed path exists for an arbitrary pair of nodes in the component.

IN Nodes from which the GSCC is reached via directed paths.

OUT Nodes that are reachable from the GSCC via directed paths.

TE "Tendrils": the rest of GWCC

Therefore, we have the components such that

$$\text{GWCC} = \text{GSCC} + \text{IN} + \text{OUT} + \text{TE} \tag{1}$$

For our data of the entire network with $N = 30,613$ nodes and $M = 280,864$ links, the GWCC component comprises 30,225 (99.0%) nodes and 280,598 (99.9%) links. The components of GSCC, IN, and OUT are summarized in Table 4. As can be seen, nearly 40% of the accounts are inside GSCC. Further, 15% of the accounts are in the upstream portion or IN, whereas 37% are in the downstream portion or OUT. These figures are very similar to those observed in the production network in Japan in a previous study [11].

The set of three components of GSCC, IN, and OUT is usually referred to as a "bowtie"; however, we find that the entire shape does not look like a "bowtie" but like a "walnut" in the sense that IN and OUT are two mutually disjoint thin skins enveloping the core of GSCC rather than two wings elongating from the center of a bowtie. In fact, by examining the shortest-path lengths from GSCC to IN or OUT, we can see that the accounts in the IN and OUT components are just a few steps away from GSCC as shown in Table 5. This feature is also similar to the production network on a nationwide scale (see the walnut structure in [11]); however, is different from many social and technological networks such as the Internet, where the maximum distances from GSCC to IN or OUT are usually very long (see the original paper [12]).

Let us remark that generally speaking, even if a network has a walnut shape in its bowtie structure, a subgraph can have a totally different shape. To illustrate, let us consider the production network which was studied in our previous paper on walnut shape [11]. The production network comprising of a million firms has such a walnut structure. Extract a subgraph for the firms in the industrial sector of construction. While the entire network's IN/OUT are typically 2

or 3-steps from its SCC, the subgraph's IN/OUT are 6-steps or even more from its SCC, implying that the latter has a "bowtie" rather than a "walnut" shape. This fact tells us that the sector of construction has a relatively elongated line of production, presumably comprising of major companies with their families of subcontractors, sub-sub contractors, and so forth. In the present case, the firms are located in a prefecture, so the money flow among them can be considered as a subgraph of the nation-wide network of production. It is a non-trivial question whether such a subgraph has a bowtie structure similar to the entire network or not.

Table 4: **Bowtie or "walnut" structure: size of each component.**

Component	**#accounts**	**Ratio(%)**
GSCC	11,543	38.2%
IN	4,508	14.9%
OUT	11,270	37.3%
TE	2,904	9.6%
total	30,225	100%

"Ratio" refers to the ratio of the number of firms to the total number of accounts in GWCC.

Table 5: **"Walnut" structure: shortest distance from GSCC to IN/OUT.**

IN to GSCC			**OUT from GSCC**		
Distance	**#accounts**	**Ratio(%)**	**Distance**	**#accounts**	**Ratio(%)**
1	4,346	96.41%	1	11,051	98.06%
2	144	3.19%	2	208	1.85%
3	8	0.18%	3	11	0.10%
4	10	0.22%	4	0	0.00%
Total	4,508	100%	Total	11,270	100%

The left half lists the number of accounts in the IN component connected to the GSCC accounts with the shortest distances within 4 at most. The right half represents the OUT component similarly.

3.4 Hodge decomposition: upstream/downstream flow

Our analysis of the bowtie structure implies that the nodes in IN and OUT are located in the upstream and downstream sides in the flow of money. The Hodge decomposition of the flow in a network is a mathematical method of ranking nodes according to their locations upstream or downstream of the flow [15]. This method, also known as the Helmholtz–Hodge–Kodaira decomposition, has been used to find such a structure in complex networks (see, e.g., neural networks [16] and economic networks [17, 18, 19]).

First, we recapitulate the method in a manner suitable for our purpose here.

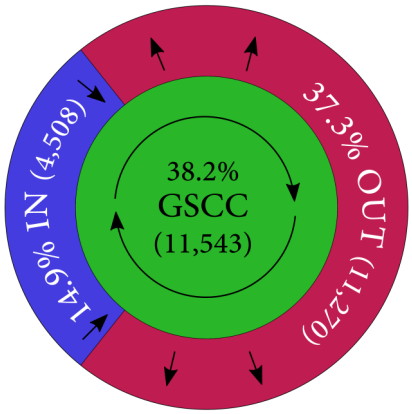

Figure 7: **Walnut structure: a schematic view.** The so-called bowtie structure reveals that GSCC includes nearly 40% of all the nodes or accounts, while the IN and OUT components include 15% and 37%, respectively (see Table 4 for the details). The prominent features are as follows. (i) The shortest distances to IN and OUT from GSCC are quite small, typically 1 or 2, and 4 at most (Table 5); hence, the ties are not elongated like a "bowtie" but rather like a "walnut" skin. (ii) The nodes in the components of IN and OUT are connected to the nodes scattered widely in GSCC. See also the study of a supplier-customer network [11] with similar features.

Let A_{ij} denote adjacency matrix of our directed network of bank transfers, i.e.,

$$A_{ij} = \begin{cases} 1 & \text{if there is a link of transfer from account } i \text{ to } j, \\ 0 & \text{otherwise.} \end{cases} \tag{2}$$

Recall that the numbers of accounts and links are N and M, respectively. We excluded all the self-loops, implying that $A_{ii} = 0$. Each link has a flow, denoted by $\tilde{F}_{ij}$, either of the total amount of transfers, f_{ij}, or the frequency of transfers, g_{ij} (see Fig. 1), i.e.,

$$\tilde{F}_{ij} = \begin{cases} f_{ij} \text{ or } g_{ij} & \text{if } A_{ij} = 1, \\ 0 & \text{otherwise.} \end{cases} \tag{3}$$

Note that there may be a pair of accounts such that $A_{ij} = A_{ji} = 1$ and $\tilde{F}_{ij}, \tilde{F}_{ji} > 0$. Next, we shall take the frequency of transfers, g_{ij}, by assuming that it represents the strength of the link.

Let us define a "net flow" F_{ij} by

$$F_{ij} = \tilde{F}_{ij} - \tilde{F}_{ji} \tag{4}$$

and a "net weight" w_{ij} by

$$w_{ij} = A_{ij} + A_{ji}. \tag{5}$$

Note that w_{ij} is symmetric, i.e., $w_{ij} = w_{ji}$, and non-negative, i.e., $w_{ij} \geq 0$ for any pair of i and j. We remark that Eq. (5) is simply a convention to consider the effect of mutual links between i and j. One could multiply Eq. (5) by 0.5

or an arbitrary positive number, which does not change the result significantly for a large network.

Now, the Hodge decomposition is given by

$$F_{ij} = F_{ij}^{(\mathrm{c})} + F_{ij}^{(\mathrm{g})}, \tag{6}$$

where the *circular flow* $F_{ij}^{(\mathrm{c})}$ satisfies

$$\sum_j F_{ij}^{(\mathrm{c})} = 0, \tag{7}$$

which implies that the circular flow is divergence-free. The *gradient flow* $F_{ij}^{(\mathrm{g})}$ can be expressed as

$$F_{ij}^{(\mathrm{g})} = w_{ij}(\phi_i - \phi_j), \tag{8}$$

i.e., the difference of "potentials". In this manner, the weight w_{ij} serves to make the gradient flow possible only where a link exists. We refer to the quantity ϕ_i as the *Hodge potential*. If ϕ_i is relatively large, the account i is located in the upstream side of the entire network, while a small ϕ_i implies that i is located in the downstream side of the entire network.

Eqs. (6)–(8) can be solved as follows. First, we combine them into the following equation for the Hodge potentials $(\phi_1, \cdots, \phi_N)(\equiv \boldsymbol{\phi})$:

$$\sum_j L_{ij}\phi_j = \sum_j F_{ij} \ , \tag{9}$$

for $i = 1, \ldots, N$. Here, L_{ij} is the so-called graph Laplacian and defined by

$$L_{ij} = \delta_{ij} \sum_k w_{ik} - w_{ij} \ , \tag{10}$$

where δ_{ij} is the Kronecker delta.

It is straightforward to show that the matrix $L = (L_{ij})$ has only one zero mode (eigenvector with zero eigenvalue), i.e., $\boldsymbol{\phi} = (1, 1, \cdots, 1)/\sqrt{N}$. The presence of this zero mode simply corresponds to the arbitrariness in the origin of ϕ. We can show that all the other eigenvalues are positive (see, e.g., [20]). Therefore, Eq. (9) can be solved for the potentials by fixing the potentials' origin. We assume that the average value of ϕ is zero, i.e., $\sum_i \phi_i = 0$.

We note that the Hodge decomposition described above plays an essential role in deciphering structure of the entire network, as well as the position and the role of each nodes in it. In studying the nodes, one may think of simply evaluating the cumulative out-flows and use it in place of the Hodge potential. This, however, misses the whole point of studying the network: Let us think of two nodes in the IN component, who have the same total out-flow. If we use the total out-flow as a measure of their locations, they are at an equal level, regardless of to whom they are connected: even if one is connected to a GSCC node close to the IN side and the other is connected to a GSCC node close to the OUT side. This also applies to those GSCC nodes in a reverse way: in evaluating the location of those GSCC nodes it is important to whom in the IN?OUT component they are connected. The Hodge decomposition solves this problem at once, as it is based on the network structure. Those IN nodes will

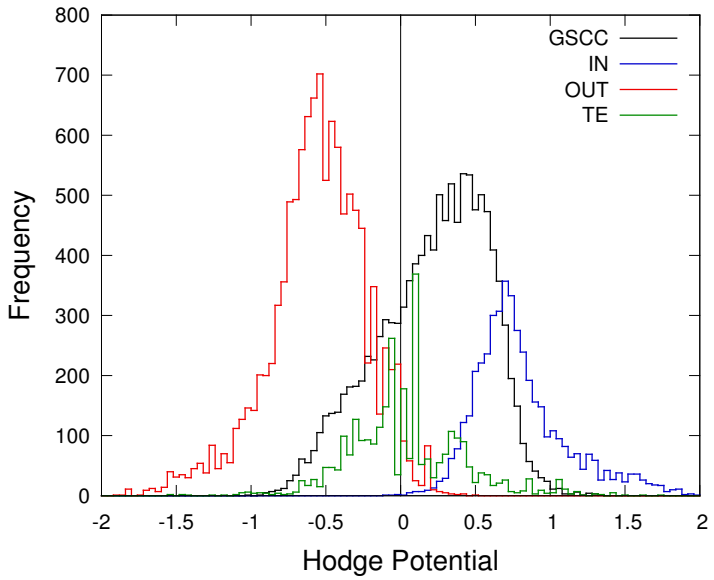

Figure 8: **Distribution of the Hodge potentials of individual accounts.** Distributions as histograms of ϕ_i in each component of the bowtie or walnut structure Fig. 7. The horizontal axis represents the value of ϕ_i of an individual node or account, while the vertical axis represents the frequency in the histogram. The black line corresponds to GSCC or the core. The blue and red lines, respectively, correspond to the IN and OUT components or upstream and downstream with respect to the core. The green line corresponds to TE (tendrils) or the rest of the nodes.

be given appropriate Hodge potential in relation with their connection to those GSCC nodes, who again are given appropriate Hodge potential with view of all the other edges of the entire network. (See Appendix A for some intuitive explanation and simple examples.)

The Hodge potentials obtained for the entire network of GWCC are shown in Fig. 8 as the distribution for the potentials of all the accounts in GWCC. By noting that the average is zero by definition, we can see that it is a bimodal distribution with two peaks at positive and negative values, while there are a number of potential values close to zero (peaks around zero). The nodes in TE (tendrils) can be considered to have locations that are not particularly relevant to upstream or downstream; we can expect that these nodes mostly have potentials close to zero, as shown by the green line, i.e., the result after deleting all the nodes contained in TE's. We can see that these TE do not contribute to large absolute values of the Hodge potentials.

It can be expected that there is a correlation between the value of the Hodge potential and the *net* amount of demand or supply of money for each node. We can measure the net amount of demand/supply by examining the in-degree and out-degree of the node, or alternatively, the in-flow and out-flow of money. Fig. 9 and Fig. 10 show the results. We find that if the potential is positive, the node is located in the upstream side, and its net degree and flow are negative. If the potential is negative, the node is located in the downstream side, and its net

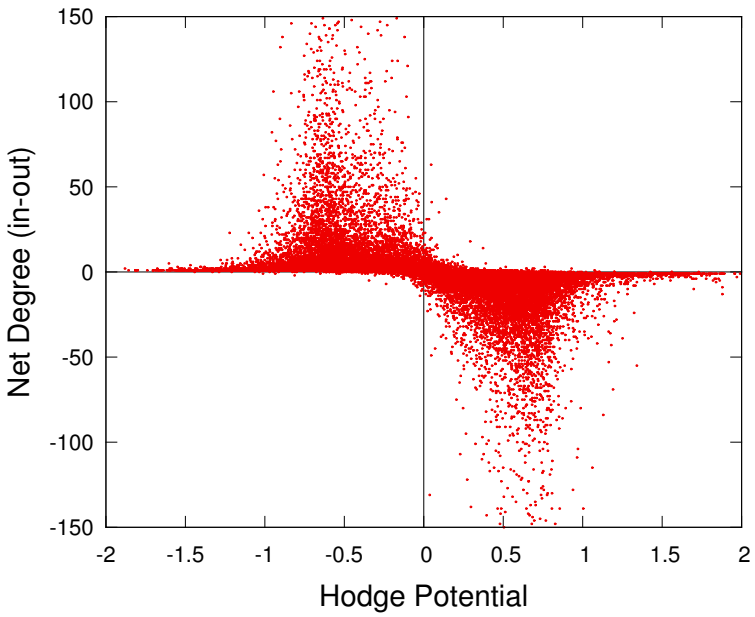

Figure 9: **Hodge potential and net degree for each node.** Each point represents a node or an account. The net degree is defined by the difference between the in-degree and the out-degree of the node. If the net degree is positive, the node has more incoming links than outgoing ones and vice versa.

degree and flow are positive.

This finding can be interpreted as follows. Consider a supplier in the production network, which supplies its products to a number of customers. The supplier has a bank account (or possibly multiple accounts) that receives money from the customers' accounts as the supplier's sales. If the supplier is in the upstream side of the supplier-customer relationship, it is likely that the account is located in the downstream side of the money flows in this study. As the supplier not only makes sales but also incurs costs, typically labor costs, there must be an outgoing flow from its account to be linked with households and other non-commercial entities, which are not included in the present study. Consequently, the supplier's account has a positive net degree and flow, while its Hodge potential is likely negative. A similar argument would hold for customers in an opposite way. In other words, our finding is a direct observation of how the flow of money reflects the economic activities among the firms' accounts.

3.5 Non-negative matrix factorization (NMF): decomposition of geographical structures of bank transfers

In this section, we focus on the geographical information of bank transfers. Each bank account has an address. We obtain the latitudes and longitudes of the bank accounts by using geocoding. Consequently, a bank transfer between two bank accounts has two coordinates of its remittance source and destination. Can geographical relations between source and destination be represented by only a small number of components of areas? We construct a non-negative matrix

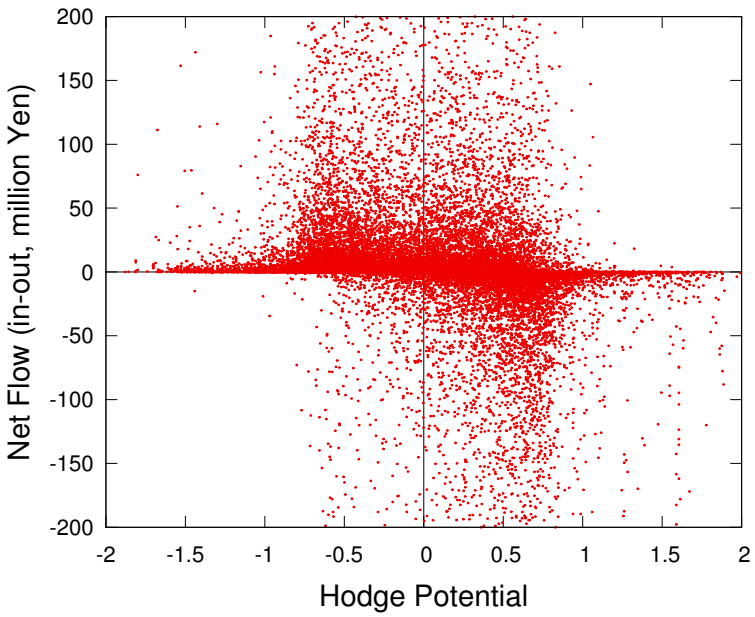

Figure 10: **Hodge potential and net flow for each node.** This figure is similar to Fig. 9 except for the vertical axis, which represents the net flow. The net flow is defined by the difference between the incoming amount of money and the outgoing one.

defined from the frequencies between the geographical areas, and we adopt NMF to find such components of geographical structures of the bank transfers.

NMF constructs an approximate factorization of a non-negative matrix [21]. Applications of NMF to real dataset give a small number of components whose linear sums can approximate elements of the dataset. For example, NMF is useful for processing facial images because it produces parts-based representations of such images [22]. To obtain the basic components whose linear sums can approximate bank transfers, we apply NMF to a non-negative matrix $V = (V_{mn})$ defined as follows. We set a square area including the prefecture and split it into $K \times K$ smaller squares in a lattice pattern, where $K = 100$. Let R_{pq} be the (p, q) small square area for $1 \leq p, q \leq K$. We consider the frequencies of bank transfers between two small square areas. Let $\alpha(p_1, q_1, p_2, q_2)$ be the frequency of bank transfers from (p_1, q_1) to (p_2, q_2) for $1 \leq p_1, q_1, p_2, q_2 \leq K$, i.e., using the frequency g_{ij} of transfers from account i to account j,

$$\alpha(p_1, q_1, p_2, q_2) = \sum_{\{(i,j)|(x_i,y_i)\in R_{p_1q_1},(x_j,y_j)\in R_{p_2q_2}\}} g_{ij}, \tag{11}$$

where (x_i, y_i) is the coordinate of the address of account i. The non-negative matrix V of size $K^2 \times K^2$ is defined by

$$V_{mn} = \log(\max\{1, \alpha(p_1, q_1, p_2, q_2)\}), \tag{12}$$

where $m = p_1 + (q_1 - 1)K$ and $n = p_2 + (q_2 - 1)K$. For practical purposes, we convert the frequencies into their logarithmic values to reduce the influence of outstanding values.

NMF gives the approximate factorization

$$V \approx WH \tag{13}$$

for some integer d, where W and H are non-negative matrices of size $K^2 \times d$ and $d \times K^2$, respectively. We assume that the approximation is based on the following minimization in which a loss function is given by the Frobenius norm:

$$\underset{W \geq 0, H \geq 0}{\operatorname{argmin}} \frac{1}{2} \sum_{m,n} (V_{mn} - (WH)_{mn})^2, \tag{14}$$

where $W \geq 0$, $H \geq 0$ means non-negativity. Technically, we solve Eq. (14) numerically with the initialization of W, H by using nonnegative double singular value decomposition (see the review [23] and references therein). The minimization yields local minima in general, but our numerical solutions under different random seeds gave essentially the same decomposition.

We let $d = 10$ from prior knowledge that the number of local communities in the prefecture is around 10. Since the mth row of V corresponds to bank transfers from (p, q) for $m = p+(q-1)K$, the rows of H constitute a basis of bank transfers for the given sources. Similarly, since the mth column corresponds to bank transfers to (p, q) for $m = p + (q - 1)K$, the columns of W constitute a basis of bank transfers for the given destinations. We can regard Eq. (13) as the approximation of V by the sum of products of these basis vectors. By letting w_m be the mth column vector and h_m be the mth row vector, we have

$$V \approx \sum_{m=1}^{d} w_m h_m. \tag{15}$$

The logarithms of the frequencies of bank transfers in the target area that are represented by V are decomposed into matrices $w_m h_m$ for $m = 1, \ldots, d$.

A basis vector v, which is a column vector w_m of W or a row vector h_m of H, can be converted to a $K \times K$ matrix $D(v)$, $1 \leq p, q \leq K$, on the geographical square area because an entry of V corresponds to the frequency of bank transfers between two small square areas. In other words, $D(v)$ is represented as a heatmap in the geographical area and Fig. 11 shows a heatmap of a basis vector. Since basis vectors seem to indicate geographically localized structures, to quantify such structures, we consider a circular area for a basis vector so that the sum of entries of the basis vector included in the circular area is maximized. Let r_{pq} be the coordinate of the center of R_{pq} and let C_{pq} be a circular area whose radius is 5 km and center is r_{pq}. Note that the radius 5 km is determined in consideration of overlappings of circles but it is not essential because the circule is not related to NMF and is used only for quantifications of geographically localized structures. For a $K \times K$ matrix $E = (E_{pq})$ and a circular area C, we define

$$\beta(C, E) = \frac{\sum_{\{(p,q)|r_{pq} \in C\}} E_{pq}}{\sum_{\{(p,q)|1 \leq p,q \leq K\}} E_{pq}}. \tag{16}$$

The proportion $\gamma(v)$ is calculated by

$$C'(v) = \underset{\{C_{pq}|1 \leq p,q \leq K\}}{\arg\max} \beta(C_{pq}, D(v)) \tag{17}$$

$$\gamma(v) = \max_{\{C_{pq}|1 \leq p,q \leq K\}} \beta(C_{pq}, D(v)). \tag{18}$$

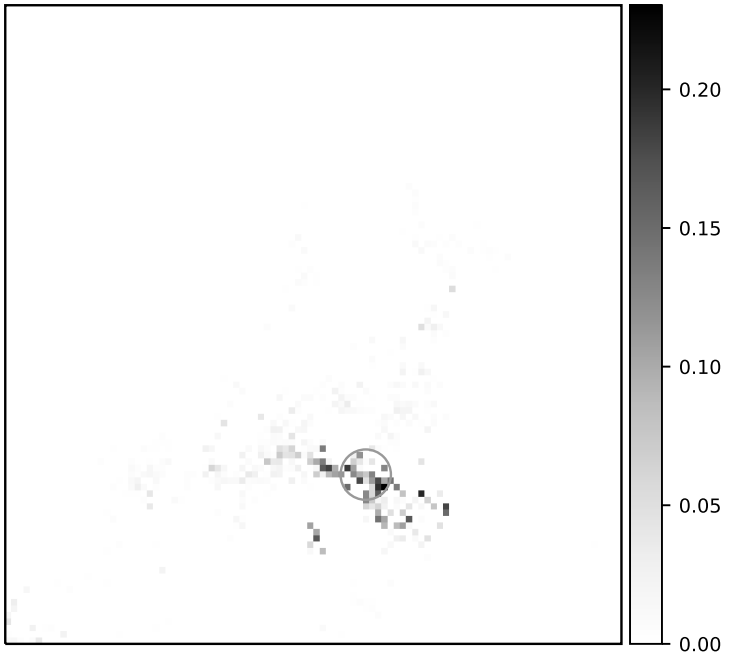

Figure 11: **Normalized basis vector obtained by NMF. The circular area has the largest sum of entries of the basis vector included in the circular area.** A normalized basis vector such that the sum of entries is one is converted into a heatmap whose lattice pattern corresponds to R_{pq}. The radius of the circular area is 5 km. The circular area is $C'(v)$ for some basis vector v, i.e., it is located at a position such that $\beta(\cdot, D(v))$ is maximized.

The proportion γ and the circular area C' of a basis vector are shown in Fig. 11.

The panels (A) and (B) in Fig. 12 show the proportions γ of all the basis vectors of sources and destinations. The proportions are more than 23% except for one basis vector in both panels of the source and destination; therefore, most basis vectors of bank transfers are localized geographically. Since the positions of the circular areas are around the centers of cities, geographically localized properties are thought to reflect the economic activity in local areas.

Fig. 12 suggests that the basis vectors of the source and destination are similar to each other. To clarify this, Fig. 13 shows a matrix of cosine similarities between a basis vector of the source and a basis vector of the destination, where the cosine similarity of w_m and h_n is calculated by

$$\frac{w_m \cdot h_n}{\|w_m\|\|h_n\|}, \tag{19}$$

where $w_m \cdot h_n$ is the inner product of w_m and h_n and $\|\cdot\|$ is the Euclidean norm of a vector. All the diagonal entries except for one are almost 1's, i.e., the mth basis vector h_m is similar to the mth basis vector w_m except for $m = 7$. These basis vectors correspond to basis vectors having geographically localized properties in Fig. 12, and the similarities of pairs of basis vectors imply that both incoming and outgoing bank transfers for a local area have similar patterns.

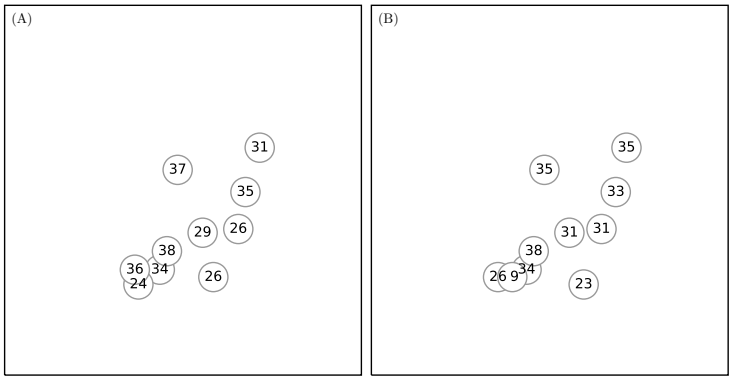

Figure 12: **Circular areas corresponding to the basis vectors and proportions of the vector entries included in the circular areas.** (A) is drawn from w_m, i.e., the basis vectors for sources, and the proportions $\gamma(w_m)$, while (B) is drawn from h_m, i.e., the basis vectors for destinations, and the proportions $\gamma(h_m)$ for $m = 1, \ldots, d$.

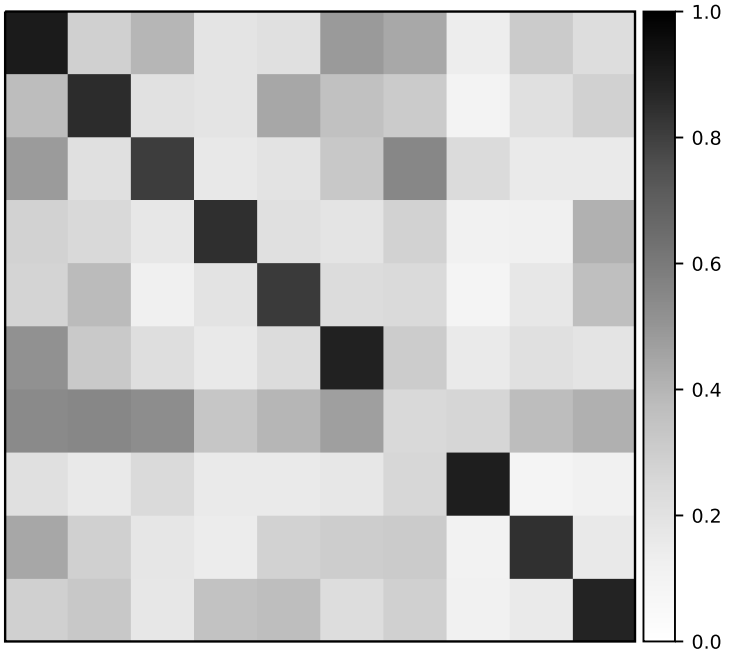

Figure 13: **Cosine similarities between basis vectors.** The vertical axis represents the indices of h_s, i.e., the sth row vector of H, and the horizontal axis represents the indices of w_t, i.e., the tth column vector of W. The index of the top left square is $(s, t) = (0, 0)$.

We can also interpret the seventh basis vectors of the source and destination that do not have similarities. The seventh basis vector of the source is localized to the largest city in the prefecture and the seventh basis vector of the destination is scattered throughout the prefecture. This means that the pair of these basis vectors corresponds to bank transfers from the largest city to the local areas. Therefore, Eq. (15) for our data gives decompositions that describe bank transfers in local areas and bank transfers between the largest city and local areas.

Finally, we state the results of NMF with different values of d. To investigate the changes in the basis vectors that occur according to d, we apply NMF to V with $d = 5, \ldots, 15$. In all the cases, most of the basis vectors are geographically localized and form source and destination pairs that are similar to each other and correspond to bank transfers in local areas. All the basis vectors are localized for d less than 7, and there is a pair of basis vectors corresponding to bank transfers between the largest city and local areas for d greater than or equal to 7. For all the values of d that we have examined, the basis vectors correspond to either bank transfers in local areas or bank transfers between the largest city and other local areas.

Geographical visualization of all the components of NMF can be found in Appendix B.

4 Conclusion

We studied an exhaustive list of bank accounts of firms and remittances from source to destination within a regional bank with a high market share of loans and deposits in a prefecture of Japan. By studying such a network of money flow, we could uncover how firms conduct the underlying economic activities as suppliers and customers from the upstream side to the downstream side of the money flow. We aggregated the remittances that occurred for each pair of accounts as a link during the period from March 2017 to July 2019 (i.e., approximately two and a half years), which comprises 30K nodes and 0.28M links. We found that the statistical features of the network are actually similar to those of a production network on a nationwide scale in Japan [3], but with greater emphasis on the regional aspects.

The bowtie analysis revealed what we refer to as a "walnut" structure in which the core and upstream/downstream components are tightly connected within the shortest distances, typically at a few steps. By quantifying the location of the individual account of a firm using the method of Hodge decomposition, we found that the Hodge potential of each node can describe the location in the entire flow of money from the upstream side to the downstream side, well characterized by the values of the potential. In particular, there is a significant correlation between the Hodge potentials and the net flows of incoming and outgoing money and links as well as the potentials and the walnut structure. This implies that we can characterize the net demand/supply of each node and decompose the flows into those due to the difference in potentials as well as divergence-free flows.

In addition, the network structure uncovered in this study can be used in predicting the default of firms. Particularly, because the financial information of small and medium-sized enterprises is often difficult to access, the credit risk

management of banks will be improved by utilizing the information obtained from the network. Information on the network structure will be also useful in promoting the regional economy because the hubs of the GSCC can be firms playing a key role in the region. Studying the network of money flow can enable the prediction of what arises following an economic shock, which is essential in economic policymaking.

Furthermore, by using non-negative matrix factorization, we uncovered the fact that the entire flow can be considered as a combination of several significant factors. One factor has a feature whereby the remittance source is localized to the largest city in the region, while the destination is scattered. The other factors correspond to the economic activities specific to different local places, which can be interpreted as local activities of the economy.

We can consider several points that remain to be studied separately from the present work. While we aggregated the entire period in this paper, it would be interesting to determine how the network changes with time by examining the time-stamps recorded in every remittance. At time scales of days, weeks, and months, it is quite likely that there are intra-day, weekly, and seasonal patterns of activities. More interestingly, under mild changes in the booms and busts of the regional economy on a relatively long time scale, the economic agents might change their behaviors possibly by changing peers in the transactions. Alternatively, under sudden changes due to natural disasters or pandemics, the agents can change their usual patterns abruptly. In other words, these are important aspects of a temporally changing network.

In addition, further investigation of the aspect of money flow amounts is warranted in the sense that the dominant driving force likely comes from "giant players" who demand or supply a large amount of money. Moreover, it would be interesting to select them in a subgraph by choosing only links with flow amounts that are larger than a certain threshold. These topics will be studied in our future work.

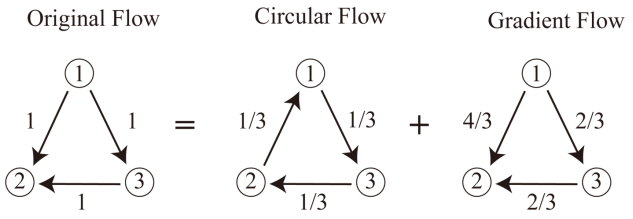

Figure A.1: A simple example.

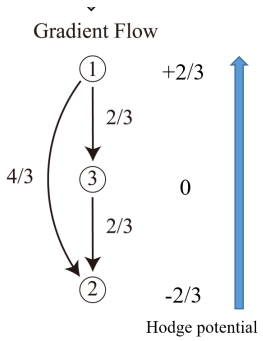

Figure A.2: The illustration of the gradient flow network, given on the most right-hand side of Fig. A.1.

A Hodge Decomposition

As is explained above, Hodge decomposition plays an essential role in studying the network structure, by allowing the researchers to quantitatively order the nodes according to their connectivity to other nodes.

One way to understand it to study some simple examples. One of the most simple but nontrivial one is illustrated in Fig. A.1. The network illustrated on the most left-hand-side ("Original Flow") is made of the three nodes with the given flow. The flows are decomposed to "Circular flow" and "Gradient Flow" as are illustrated. Sum of the two flows are equal to the original flow: For example, from the node no.1 to the node no.2, circular flow is $-1/3$ (as it is $+1/3$ in the other direction) and the gradient flow is $+4/3$, which adds up to 1, the value of the original flow. Also, the gradient flow satisfies the property (7). Furthermore, the gradient flow satisfies Eq.(8) with all the weights equal to one ($w_{ij} = 1$) and the Hodge potential $(\phi_i) = (+2/3, -2/3, 0)$. Fig. A.1 shows the visualization of this network with the use of the Hodge potential (ϕ_i) as vertical coordinate. In this illustration it is straightforward to see that gradient flows are equal to the difference of the Hodge potentials of the relevant nodes.

Fig. A.3 and Fig. A.4 are simple and more illustrative examples, where all flows are of strength 1 as in the first example. In both Figures, on the left panel is the visualization of the whole network by using the spring-charge method, and on the right panel is the visualization of the same network with the horizontal coordinate determined by the Hodge potential and the horizontal coordinate determined by the spring-charge method.

In Fig. A.3, the nodes are placed in a left-right symmetric manner on the

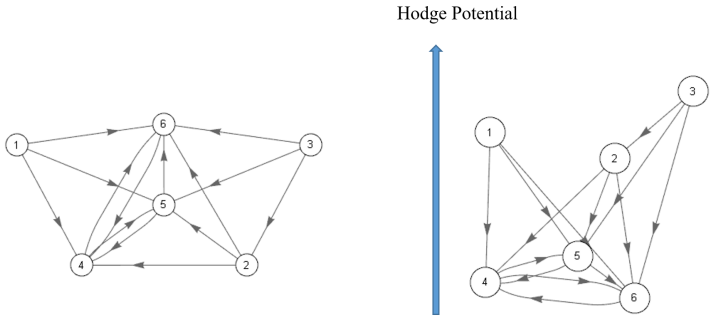

Figure A.3: A sample network. On the left-hand side is visualization by the charge-spring visualization and on the right-hand-side is the visualization of the same network with the horizontal coordinates determined by the Hodge potential and the horizontal coordinate determined by the spring-charge method.

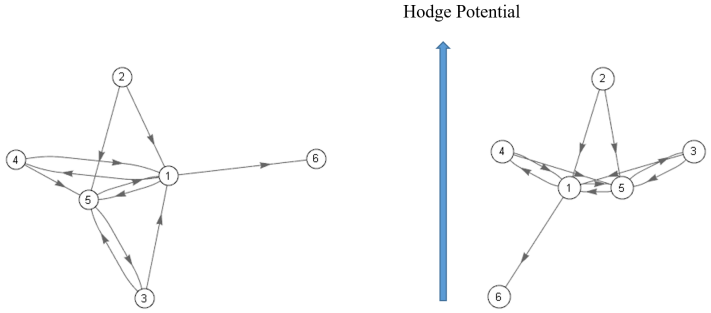

Figure A.4: Another sample network, visualized in the same manner as in Fig. A.3.

left panel, although the links do not have the same symmetry. The nodes no.1 and no.3 are placed in same vertical position. If one used the total out-flow as a measure of the rank, they would be placed just like this, as both of them have the total out-flow equal to three. The right panel, however, shows a different picture: Nodes no.1 and no.3 are placed at different heights, due to the difference in their Hodge potential, which again is due to the difference in the way they are connected to other nodes.

The example in Fig. A.3 shows the power of the Hodge decomposition in a different manner: On the left-panel, we do not see any symmetry and the roles of the nodes are not apparent. On the contrary, the right panels shows the left-right symmetry except for the node no.6. Nodes no.1 and no.5 plays very similar role in this network, the only difference being that no.1 is connected to no.6. Same is true for the nodes no.4 and no.3. Without the use of the Hodge decomposition this fact is rather difficult to see.

As seen in these examples, the Hodge potential plays an important role in clarifying the whole structure of the network.

B NMF Components and Geographical Locations

In Section 3.5, we constructed a non-negative matrix defined from the frequencies between the geographical areas, and applied NMF (non-negative matrix factorization) to find components of geographical structures of the bank transfers. It would be helpful to show how the resulting components are located geographically by actually displaying in the map of Shiga prefecture and its neighboring region of Kyoto.

Recall from (12) that V_{mn} represents the strength of remittance from area m to n, where the strength was defined by the logarithm of frequency of remittance. NMF decomposes the matrix as (13), or explicitly

$$V_{mn} \approx \sum_{k=1}^{d} W_{mk} H_{kn}, \tag{B.1}$$

where d was the number of components. d is much smaller than the dimension of the matrix V_{mn} in row and column, each being K^2, namely the square of the number of mesh in each direction. Our results correspond to $d = 10$.

For each $k = 1, 2, \ldots, d$, the column vector $W_{\cdot k}$ represents how remittance takes place in its source in the component of k, while the row vector $H_{k\cdot}$ represents how remittance takes place in its destination in the k-th component. It is then possible to visualize source and destination for each component in a geographical map by plotting these basis vectors.

Fig. B.1 (a) to (d) depict all the components for $k = 1, 2, \ldots, d$. Each pair in a rectangle displays the pair of source and destination, $W_{\cdot k}$ and $H_{k\cdot}$. From Fig. B.1 (a) to (c), we can observe that the source and destination are mostly concentrated in a particular area shown by a circle. Examination of cities in the prefecture tells us that those concentrated area correspond to cities, which are annotated with city names in the plots. For example, the bottom pair in Fig. B.1 (a) shows that the source and destination are located in the Otsu city, the most populated city in the prefecture. Therefore, each of these components represents remittance inside the corresponding city and their surrounding regional area.

On the other hand, Fig. B.1 (d) is the remaining component, which shows that the source is concentrated in the Otsu city, while the destination is scattered all over the cities of the prefecture and also over the area of Kyoto city in the neighboring prefecture of Kyoto. This component is quite different from the other ones in the asymmetric role of source and destination. Recall that the cosine similarities between basis vectors in Fig. 13 precisely shows these facts.

We also show the same plot of Fig. 12 over the same map in Fig. B.2 for the benefit of the readers.

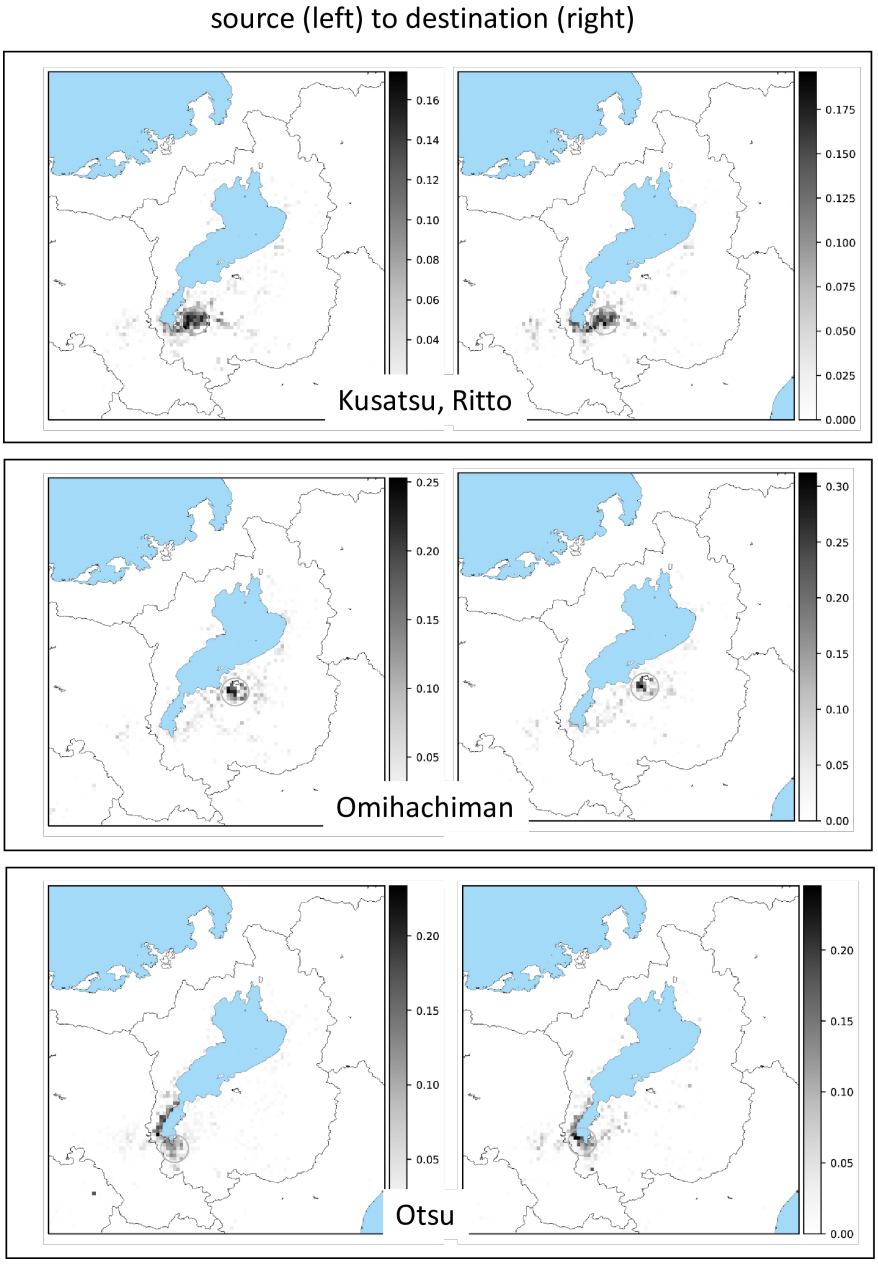

(a) Three components taken from the $d = 10$ components.

Figure B.1: Source and desination of each component

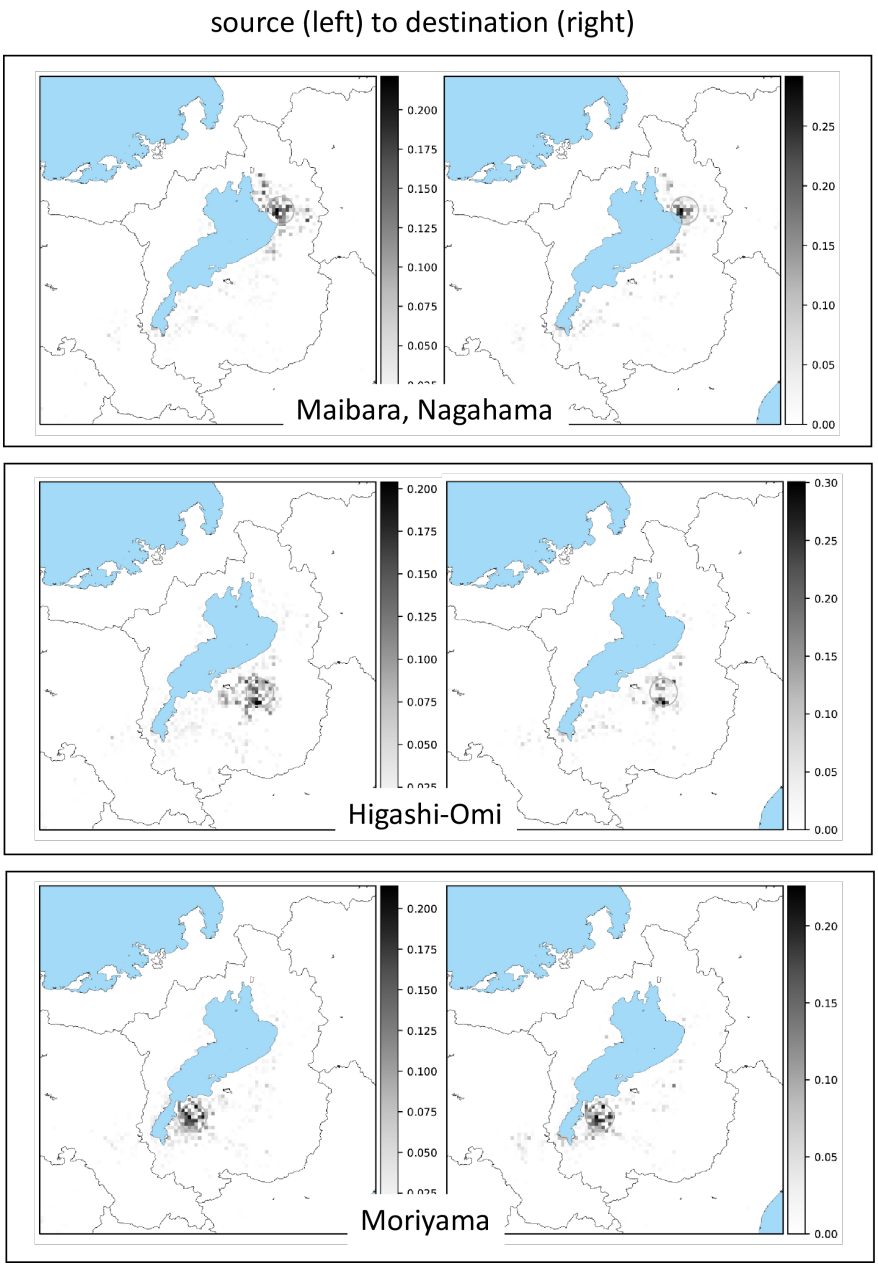

(b) Three components taken from the $d = 10$ components.

Figure B.1: Source and desination of each component (Continued)

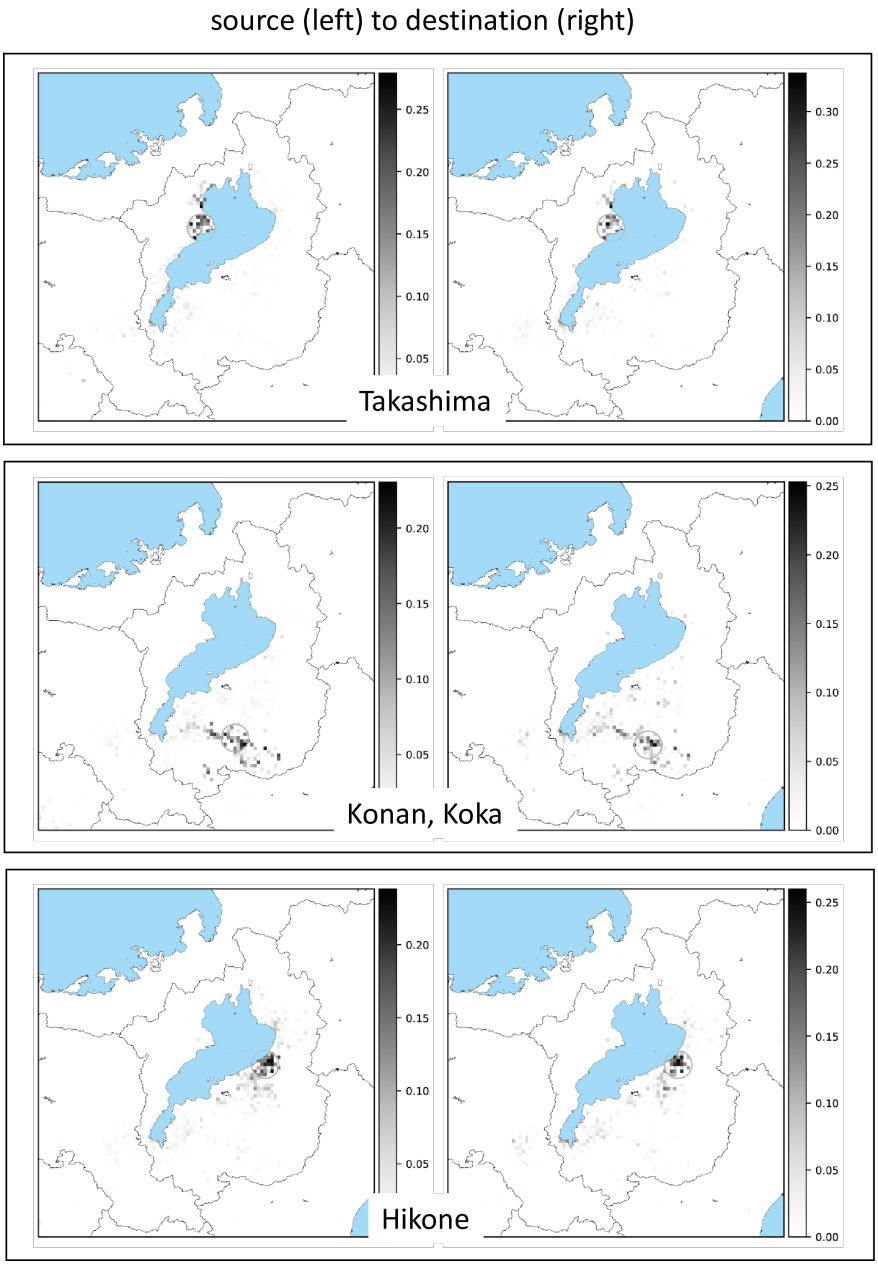

(c) Three components taken from the $d = 10$ components.

Figure B.1: Source and desination of each component (Continued)

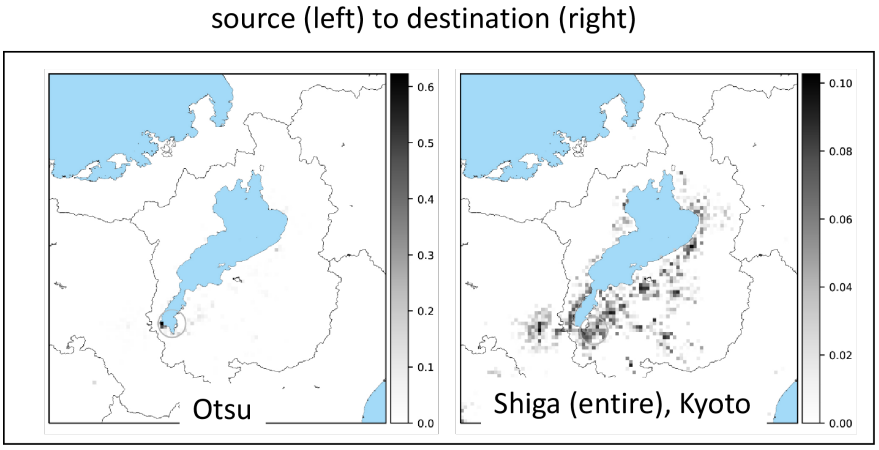

(d) One component taken from the $d = 10$ components.

Figure B.1: Source and desination of each component (Continued)

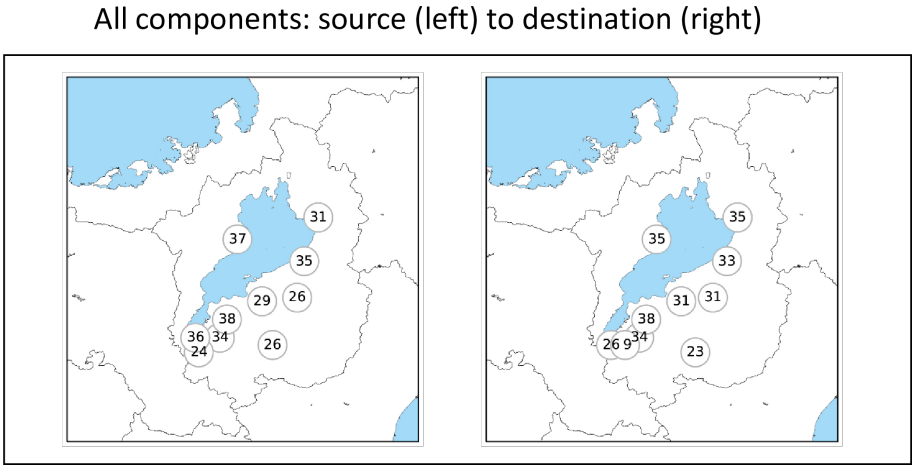

Figure B.2: Fig. 12 is depicted in a geographical map. There are $d = 10$ circles corresponding to the components. Each number in a circle represents how each basic vector is concentrated to the circle in the components of the vector (in percentage).

Acknowledgements

This study is conducted as a part of the Project "Macro-Economy under COVID-19 influence: Data-intensive analysis and the road to recovery" undertaken at the Research Institute of Economy, Trade and Industry (RIETI). The authors are grateful to Shiga Bank, Ltd. for giving us an opportunity to study such a unique and valuable dataset. They are also grateful to Yoshiaki Nakagawa (The Center for Data Science Education and Research, Shiga University) and Discussion Paper seminar participants at RIETI for helpful discussions.

This work was supported in part by MEXT as Exploratory Challenges on Post-K computer (Studies of Multi-level Spatiotemporal Simulation of Socioeconomic Phenomena), the project "Large-scale Simulation and Analysis of Economic Network for Macro Prudential Policy" undertaken at the Research Institute of Economy, Trade and Industry (RIETI), and JSPS KAKENHI Grant Numbers 17H02041, 19K22032, and 20H02391.

References

[1] Bank of japan: Guide to japan's flow of funds accounts. `https://www.boj.or.jp/en/statistics/`. accessed June 2020.

[2] Oecd: Input-output tables. `http://www.oecd.org/sti/ind/input-outputtables.htm`. accessed June 2020.

[3] Hideaki Aoyama, Yoshi Fujiwara, Yuichi Ikeda, Hiroshi Iyetomi, Wataru Souma, and Hiroshi Yoshikawa. *Macro-Econophysics – New studies on Economic Networks and Synchronization*. Cambridge University Press, Cambridge, UK, 2017.

[4] Hiroyasu Inoue and Yasuyuki Todo. Firm-level propagation of shocks through supply-chain networks. *Nature Sustainability*, 2:841–847, 2019.

[5] Hiroyasu Inoue and Yasuyuki Todo. The propagation of economic impacts through supply chains: The case of a mega-city lockdown to prevent the spread of covid-19. Research Institute of Economy, Trade and Industry (RIETI) Discussion Paper Series, 4 2020.

[6] Yoshi Fujiwara and Hideaki Aoyama. Large-scale structure of a nationwide production network. *The European Physical Journal B*, 77(4):565–580, 2010.

[7] Takayuki Yamaguchi, Kazuma Tsuji, Yoshiaki Nakagawa, Takuma Tanaka, and Kentaro Kikuchi. Sector-wise impact of COVID-19 pandemic on transactions among firms: a real-time analysis of financial big data. The Institute for Economics & Business Research Discussion Paper Series J-1. `https://www.econ.shiga-u.ac.jp/ebrisk/DPJ1Yamaguchi.pdf` [in Japanese].

[8] Albert-László Barabási. *Network science*. Cambridge University Press, Cambridge, UK, 2016.

[9] Martin Rosvall and Carl T Bergstrom. Maps of random walks on complex networks reveal community structure. *Proceedings of the National Academy of Sciences*, 105(4):1118–1123, 2008.

[10] Martin Rosvall and Carl T Bergstrom. Multilevel compression of random walks on networks reveals hierarchical organization in large integrated systems. *PloS one*, 6(4):e18209, 2011.

[11] Abhijit Chakraborty, Yuichi Kichikawa, Takashi Iino, Hiroshi Iyetomi, Hiroyasu Inoue, Yoshi Fujiwara, and Hideaki Aoyama. Hierarchical communities in walnut structure of japanese production network. *PLoS ONE*, 13(8):DOI: 10.1371/journal.pone.0202739, 2018.

[12] A. Broder, R. Kumar, F. Maghoul, P. Raghavan, S. Rajagopalan, R. Stata, A. Tomkins, and J. Wiener. Graph structure in the Web. *Computer Networks*, 33(1-6):309–320, 2000.

[13] D. Krackhardt and J. R. Hanson. Informal networks. *Harvard Business Review*, 71(4):104–111.

[14] D'Errico, Marco and Battiston, Stefano and Peltonen, Tuomas and Scheicher, Martin. How does risk flow in the credit default swap market? Working Paper Series No. 2041, European Central Bank, March 2017.

[15] X. Jiang, L.-H. Lim, Y. Yao, and Y. Ye. Statistical ranking and combinatorial hodge theory. *Mathematical Programming*, 127(1):203–244, 2011.

[16] K. Miura and T. Aoki. Scaling of hodge-kodaira decomposition distinguishes learning rules of neural networks. *IFAC-PapersOnLine*, 48(18):175–180, 2015. 4th IFAC Conference on Analysis and Control of Chaotic Systems CHAOS 2015.

[17] Y. Kichikawa, H. Iyetomi, T. Iino, and H. Inoue. Hierarchical and circular flow structure of interfirm transaction networks in japan. `https://ssrn.com/abstract=3173955`, May 2018.

[18] H. Iyetomi, H. Aoyama, Y. Fujiwara, W. Souma, I. Vodenska, and H. Yoshikawa. Relationship between macroeconomic indicators and economic cycles in u.s. *Sci. Rep.*, 10:8420, 2020. https://doi.org/10.1038/s41598-020-65002-3.

[19] RS MacKay, S Johnson, and B Sansom. How directed is a directed network? *arXiv preprint arXiv:2001.05173*, 2020.

[20] Y. Fujiwara and R. Islam. Hodge decomposition of bitcoin money flow, 2020. in press.

[21] Daniel D. Lee and H. Sebastian Seung. Algorithms for non-negative matrix factorization. In *Proceedings of the 13th International Conference on Neural Information Processing Systems*, NIPS'00, pages 535–541, Cambridge, MA, USA, 2000. MIT Press.

[22] Daniel D. Lee and H. Sebastian Seung. Learning the parts of objects by non-negative matrix factorization. *Nature*, 401(6755):788–791, 1999.

[23] Michael W. Berry, Murray Browne, Amy N. Langville, V. Paul Pauca, and Robert J. Plemmons. Algorithms and applications for approximate nonnegative matrix factorization. *Computational Statistics & Data Analysis*, 52(1):155–173, 2007.